RESEARCH ARTICLE

Key Points:
- The first comparative study on the solar and interplanetary characteristics of moderate storms during solar cycles 23 and 24
- The contribution of moderate storms toward reduced geoeffectiveness in solar cycle 24 is examined
- The correlation between VBz and Dst is determined, and the magnetospheric response is determined for the cycles 23 and 24

Correspondence to:
R. Selvakumaran,
selva2986@gmail.com

On the reduced geoeffectiveness of solar cycle 24: A moderate storm perspective

R. Selvakumaran[1], B. Veenadhari[1], S. Akiyama[2,3], Megha Pandya[1], N. Gopalswamy[2], S. Yashiro[2,3], Sandeep Kumar[1], P. Mäkelä[2,3], and H. Xie[2,3]

[1]Indian Institute of Geomagnetism, New Panvel, India, [2]Solar Physics Laboratory, NASA Goddard Space Flight Center, Greenbelt, Maryland, USA, [3]Department of Physics, Catholic University of America, Washington, District of Columbia, USA

Abstract The moderate and intense geomagnetic storms are identified for the first 77 months of solar cycles 23 and 24. The solar sources responsible for the moderate geomagnetic storms are indentified during the same epoch for both the cycles. Solar cycle 24 has shown nearly 80% reduction in the occurrence of intense storms whereas it is only 40% in case of moderate storms when compared to previous cycle. The solar and interplanetary characteristics of the moderate storms driven by coronal mass ejection (CME) are compared for solar cycles 23 and 24 in order to see reduction in geoeffectiveness has anything to do with the occurrence of moderate storm. Though there is reduction in the occurrence of moderate storms, the Dst distribution does not show much difference. Similarly, the solar source parameters like CME speed, mass, and width did not show any significant variation in the average values as well as the distribution. The correlation between VB_z and Dst is determined, and it is found to be moderate with value of 0.68 for cycle 23 and 0.61 for cycle 24. The magnetospheric energy flux parameter epsilon (ε) is estimated during the main phase of all moderate storms during solar cycles 23 and 24. The energy transfer decreased in solar cycle 24 when compared to cycle 23. These results are significantly different when all geomagnetic storms are taken into consideration for both the solar cycles.

1. Introduction

Geomagnetic storms are major disturbances in the Earth's magnetosphere caused by energetic solar wind magnetic structures impacting and injecting material into the magnetosphere by the process of reconnection [*Dungey*, 1961; *Gonzalez et al.*, 1994]. Geomagnetic storms are marked by a decrease in the horizontal intensity of the Earth's magnetic field, which results from ring current enhancement due to the increase in the population of magnetopsheric trapped particles [*Chapman and Bartels*, 1940; *Gonzalez et al.*, 1994]. Geomagnetic storms are caused by southward interplanetary magnetic field (IMF) that allows efficient energy transfer from the solar wind into the Earth's magnetosphere [*Dungey*, 1961; *Gonzalez and Tsurutani*, 1987; *Gonzalez et al.*, 1994; *Echer et al.*, 2005; *Echer et al.*, 2013]. It is now well understood that geomagnetic storms are caused by coronal mass ejections (CMEs) and corotating interaction regions (CIRs) originating from the Sun that evolves through the interplanetary medium before impacting the magnetosphere [*Brueckner et al.*, 1998; *Webb et al.*, 2001; *Berdichevsky et al.*, 2002; *Zhang et al.*, 2003; *dal Lago et al.*, 2004; *Zhang et al.*, 2007; *Gopalswamy et al.*, 2007; *Gopalswamy*, 2010]. CMEs cause severe storms while CIRs cause moderate storms [*Gosling et al.*, 1991; *Tsurutani and Gonzalez*, 1997; *Richardson et al.*, 2002; *Tsurutani et al.*, 2006; *Gopalswamy*, 2008; *Zhang et al.*, 2007]. The counterpart of CMEs in the interplanetary medium is termed as interplanetary coronal mass ejections (ICMEs), which are usually categorized as magnetic clouds (MCs) and nonmagnetic clouds or ejecta (EJ) based on their in situ plasma and magnetic signatures [*Klein and Burlaga*, 1982; *Gopalswamy et al.*, 2010a, 2010b; *Riley and Richardson*, 2012, and references therein]. CIRs develop when high-speed solar wind streams (HSSs) emanating from coronal holes interact with streams of lower speed. CIRs consist of enhanced density and magnetic field, which when associated with southward IMF result in geomagnetic storms [*Smith & Wolf*, 1976; *Gosling*, 1996; *Gosling and Pizzo*, 1999].

The type of interplanetary (IP) structure causing geomagnetic storms varies with the solar cycle: CME-associated storms dominate during solar maxima, whereas CIR storms mostly occur during the declining phase of solar cycles [*Webb*, 1991; *Yashiro et al.*, 2004; *Mursula and Zieger*, 1996]. Geomagnetic storms result in intense currents in the magnetosphere, changes in the radiation belts, and heating of the ionosphere and upper atmospheric region. Geomagnetic disturbances are measured using a variety of indices, one of which

is the Disturbance storm time (Dst) index [*Sugiura*, 1964]. The Dst index represents changes in the magnetic field caused by magnetopsheric currents such as the ring current, tail current, asymmetric ring current, and magnetopause current [*Alexeev et al.*, 1996; *Daglis and Thorne*, 1999; *Turner et al.*, 2000; *Liemohn et al.*, 2001; *Lopez et al.*, 2015]. Using Dst, geomagnetic storms are classified as weak ($-30 < Dst < -50$ nT), moderate ($-50 < Dst < -100$ nT), and intense ($Dst < -100$ nT) [*Gonzalez et al.*, 1994; *Sugiura and Chapman*, 1960].

There are several studies on intense geomagnetic storms and the associated solar sources and the interplanetary conditions [*Tsurutani et al.*, 1988, 1992, 1995, 2006; *Gonzalez et al.*, 1999, 2007, 2011; *Gonzalez and Echer*, 2005; *Zhang et al.*, 2006, 2007; *Echer et al.*, 2008a, 2008b]. The magnetosphere-solar wind coupling has also been considered using the energy flux parameter epsilon (ε) for severe geomagnetic storms [*Perrault and Akasofu*, 1978; *Nishida*, 1983; *Mac-Mahon and Gonzalez*, 1997; *Holzer and Slavin*, 1979; *Sibeck et al.*, 1991; *Alex et al.*, 2006]. The ε parameter gives the maximum energy transferred to the magnetosphere from the solar wind during the geomagnetic storms, and it is highly dependent on the magnetic field component and the solar wind velocity. The solar wind-magnetosphere dynamo is generated during the interaction of IMF with the magnetosphere, and the energy transfer is in the range of 10^{12}–10^{13} W during geomagnetic storms [*Weiss et al.*, 1992; *Mac-Mahon and Gonzalez*, 1997; *Alex et al.*, 2006].

As the Sun emerged from the deep solar minimum to the rising phase of the solar cycle 24, the sunspot number (SSN) was relatively small [*Gopalswamy et al.*, 2012; *Solomon et al.*, 2013; *Lean et al.*, 2014; *Potgieter et al.*, 2014; *Kilpua et al.*, 2014]. Although SSN decreased by 40% in solar cycle 24, the CME rate was similar to that in cycle 23 [*Gopalswamy et al.*, 2014]. There is not much diminution observed in the number of halo CMEs, which are generally more geoeffective. However, there was a severe reduction in the geoeffectiveness of CMEs as indicated by the drastic decrease in the number of intense geomagnetic storms during solar cycle 24. An average reduction in Dst from -66 to -55 nT was found for MC-associated storms during the first 73 months of solar cycle 24 compared to the same epoch in cycle 23. This has been attributed to the anomalous expansion of CME in the current solar cycle [*Gopalswamy et al.*, 2015a]. In another study [*Gopalswamy et al.*, 2015b] a significant reduction in CME mass and increase in CME width for limb CMEs are found in solar cycle 24 when compared to cycle 23.

While the reduction in intense storms is clear, it is of interest to know what happens to moderate storms. Although there are other works on cycle 23 moderate storms [*Tsurutani and Gonzalez*, 1997; *Wang et al.*, 2003; *Zhang et al.*, 2006; *Xu et al.*, 2009; *Echer et al.*, 2011, 2013; *Hutchinson et al.*, 2011; *Tsurutani et al.*, 2011], there is no comparative study between solar cycles 23 and 24. This work attempts to see if there is any change in the occurrence of moderate storms between solar cycles 23 and 24. This work involves the identification of the source of the moderate geomagnetic storms in solar cycles 23 and 24 and comparison of the interplanetary parameters and the response of magnetosphere related to moderate storms.

2. Data and Observations

This study concerns moderate geomagnetic storms that occurred during the first 77 months of cycles 23 (1 May 1996 to 30 September 2002) and 24 (1 September 2008 to 31 January 2015). Based on the availability, final, provisional, and real-time Dst values are obtained from (http://wdc.kugi.kyoto-u.ac.jp/index. html). The Dst values are carefully examined to identify moderate storms by eliminating Dst excursions due to prior geomagnetic storms in progress. Only occurrences when a prior storm recovered up to 80% have been considered. We use the source CME identification for solar cycle 23 reported in the interplanetary (IP) shock catalog by *Gopalswamy et al.* [2010a] and the list provided by *Richardson and Cane* [2010] online (http://www.srl.caltech.edu/ACE/ASC/DATA/level3/ icmetable2.htm). For cycle 24, the CMEs are identified by running movies of coronagraph images available at http://cdaw.gsfc.nasa.gov/ CME_list/index.html. A few identifications are taken from the list given by Richardson and Cane as mentioned above. The solar source location is taken from the halo CME catalog (http://cdaw.gsfc.nasa.gov/ CME_list/halo /halo.html [*Gopalswamy et al.*, 2010b]). For other CMEs we identify the solar source from the flare locations given in the online Solar Geophysical Data (SGD) report. For events not listed in SGD, the sources are identified using images from the Extreme ultraviolet Imaging Telescope on board SOHO, the Atmospheric Imaging Assembly on board the Solar Dynamics Observatory (SDO), and H-alpha observatories (as detailed in *Gopalswamy et al.* [2007]). Mass and width of the CMEs are taken from the CME catalog

Solar cycle 23

Solar cycle 24
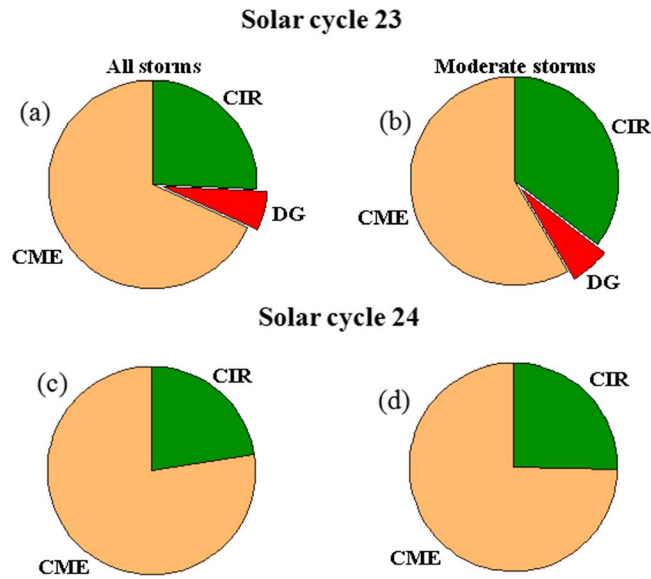
Figure 1. Distribution of CME and CIR driven for all storms and moderate storms during (a, b) SC 23 and (c, d) SC 24. DG denotes storms whose sources are unknown due to data gap.

(http://cdaw.gsfc.nasa.gov/CME_list/index.html [*Gopalswamy et al.*, 2009]). The solar wind plasma and magnetic parameters with 1 min resolution are obtained from CDAWeb (http://cda-web.gsfc.nasa.gov/cgi-bin/eval1.cgi).

Based on the *Dst* index criterion as mentioned in section 1, a total of 166 moderate and intense geomagnetic storms are identified in Solar cycles 23 and 67 in cycle 24 (hereafter all the comparisons of solar cycles 23 and 24 storms refer to the corresponding epoch of 77 months in each cycle). We see that the storm occurrence rate in cycle 24 is reduced by 57.5% compared to that in cycle 23. The monthly average SSN is ~69 and ~40 for solar cycles 23 and 24, respectively. So nearly 40% decrease is observed in SSN for solar cycle 24 when compared to solar cycle 23

[*Gopalswamy et al.*, 2014]. The storm occurrence rate reduced more than SSN did. The decrease in SSN is not sufficient to explain the observed reduction in geoeffectiveness in solar cycle 24.

Not all storm sources follow the sunspot activity, so in order to understand the relation between solar activity and the occurrence of storms it is necessary to differentiate the storms of different origin. The distribution of geomagnetic storms between CME and CIR sources is given in Figures 1a–1d for cycles 23 and 24. The combined set of intense and moderate storms is compared with the moderate storms. There was a small data gap (DG) in solar cycle 23 because there was no CME observation for a brief period (3 months in 1998 and 1 month in 1999) when the SOHO spacecraft was temporarily disabled. Apart from the data gap, five moderate storms are not included in the study. The first two occurred on 17 September 2000 and 9 October 2001. These cases are complex and no CME is detected by SOHO. No shocks are detected in situ in these events. The 17 September 2000 storm is associated with a narrow negative B_z interval. The other three occurred on 12 April 2014, 30 April 2014, and 7 January 2015 with a minimum *Dst* of −80 nT, −67 nT, and −99 nT, respectively. The 7 January 2015 is probably associated with the 4 January 2015 CME, but the confidence in the association is not high since the CME could not be tracked to 1 AU. The solar source location of the 30 April 2014 storm is identified from SDO images, but Large Angle and Spectrometric Coronagraph (LASCO) did not detect it may be because the CME was too narrow. No STEREO observations exist during this period, making it difficult to trace the CME at 1 AU.

The CME-driven storms are examined based on the ICME structure observed at 1 AU. Similarly, CIR-associated storms are identified by examining the variation in total magnetic field, proton temperature, and density at 1 AU. Table 1 gives the statistics on the moderate and intense storms occurring in the two cycles. From Table 1 and Figure 1 it is clear that CME storms constitute the majority in both cycles. In cycle 23, out of a total 166 storms, 111 (~66.8%) are of CME origin, 43 (~25.9%) of CIR origin, and 12 (~7.2%) have a data gap. Out of the 111 moderate storms in cycle 23, 63 (56.7%) are of CME origin, 40 (36%) of CIR origin, and 8 (7.2%) have

Table 1. Intense and Moderate Storms During the First 77 Months of Cycles 23 and 24

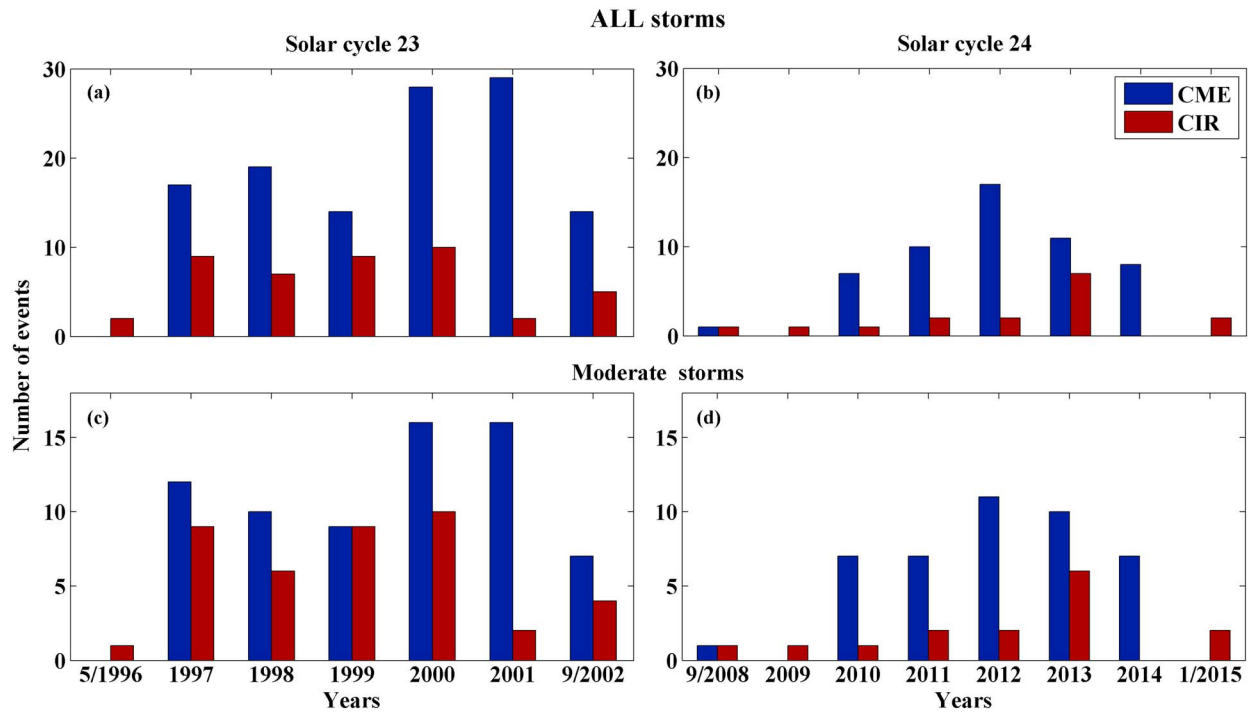|		All	Moderate	Intense
Solar cycle 23	CME	111 (66.8%)	63 (56.7%)	48 (88.8%)
	CIR	43 (25.9%)	40 (36%)	3 (5.5%)
	Data gap	12 (7.2%)	8 (7.2%)	3 (5.5%)
	Total	166	111	54
Solar cycle 24	CME	52 (77.6%)	41 (74.5)	11 (91.7%)
	CIR	15 (22.3%)	14 (25.5%)	1 (8.3%)
	Data gap	-	-	-
	Total	67	55	12

Figure 2. Yearly occurrence of CME and CIR-driven storms: All storms and moderate storms for (a, b) SC 23 and (c, d) SC 24.

a data gap. *Echer et al.* [2013] investigated 213 moderate storms from cycle 23 (1996–2008) and found that the moderate storms were due to CIRs and pure high-speed streams (HSSs) (47.9%), MCs and noncloud ICMEs (20.6%), pure sheath fields (10.8%), and sheath-ICME combination (9.9%). The difference between *Echer et al.* [2013] and our results can be attributed to the different periods considered for analysis. In solar cycle 24, ~77.6 (52 out of 67) of all storms (the combined set of intense and moderate storms) are of CME origin and only ~22.3% (15 out of 67) are of CIR origin. Considering only the moderate storms of cycle 24, we find that ~74.5% (41 out of 55) are of CME origin whereas 25.5% (14 out of 55) are of CIR origin. Table 1 also shows that there were 48 CME-driven intense storms in cycle 23 compared to only 11 in cycle 24, which corresponds to a reduction of ~78%.

Figure 2 shows the yearly distribution of CME- and CIR-driven storms grouped into all storms (a and b) and moderate storms (c and d) of cycles 23 and 24, respectively. The occurrence rate of all storms peaks around 2001 for solar cycle 23 and around 2012 for solar cycle 24 when CME-associated storms is considered. The occurrence rate of CME-associated moderate storms peaks around 2000 and sustains till 2001 in solar cycle 23 (Figure 2c). The behavior of moderate storms in cycle 24 is similar to that in cycle 23 (Figure 2d). All CIR-associated storms peak around 2000 (cycle 23) and around 2011 (cycle 24). The peak of CME storms in solar cycle 23 matches with the SSN peak. *Echer et al.* [2013] observed two different peaks in the storm occurrence rate during solar cycle 23, one in 2001 and the other during 2003–2005. The first peak is during the solar maximum phase, and the second one is in the declining phase of the cycle. Our peak matches with *Echer et al.* [2013] when source region of the moderate storms is not separated.

3. Comparison of Solar Source/Interplanetary Parameters/Magnetospheric Response of Moderate Storms

3.1. *Dst* Value and Source Location Distribution

Figure 3 shows that the distribution of *Dst* in moderate storms is narrower in solar cycle 24 than in cycle 23. Most (~68%) of the moderate storms in solar cycle 24 had *Dst* in the range of −50 nT to −75 nT. The average *Dst* values for the two cycles are comparable (~−70 nT), and though there is nearly 40% reduction observed in number of events, the average values are the same. Since we considered only moderate storms, we do not
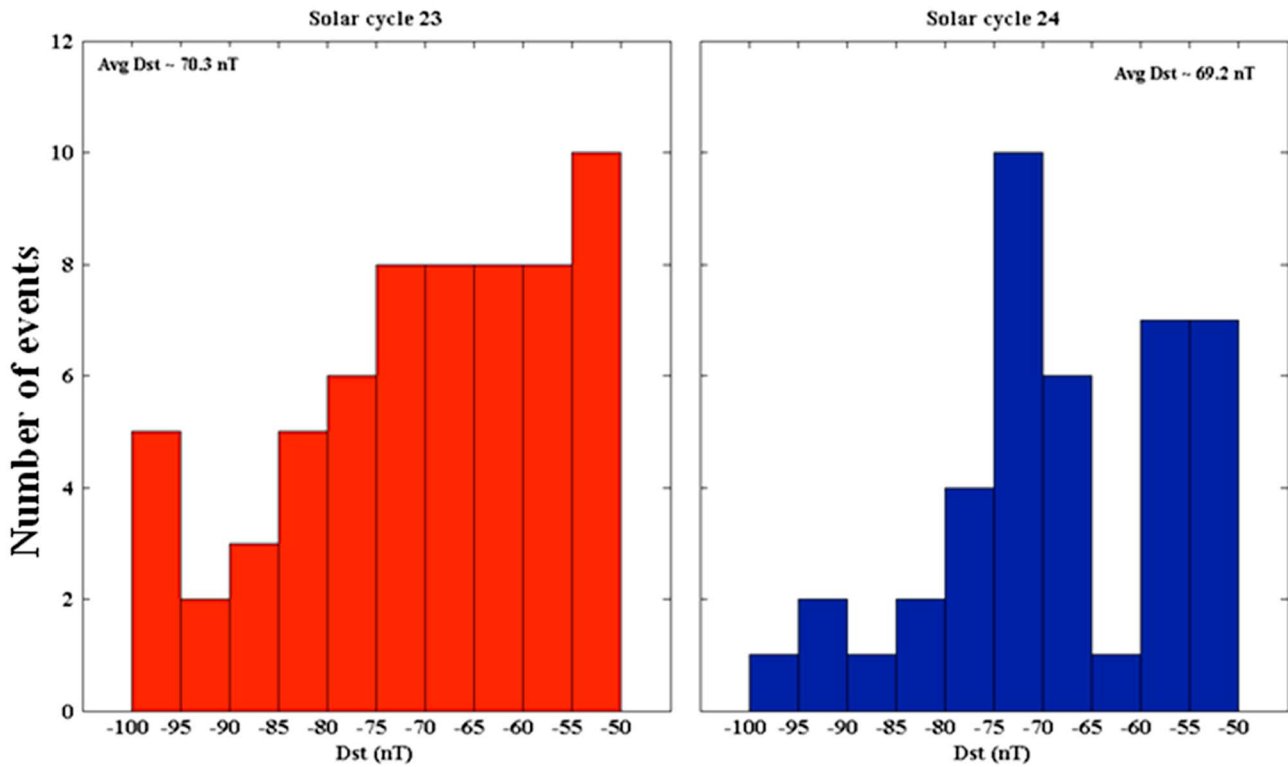
Figure 3. Distribution of *Dst* value for moderate storm occurred during SCs 23 and 24.

expect much change in the average *Dst* values. To verify whether there is significant difference in *Dst* distribution for solar cycles 23 and 24, we have used Kolmogorov-Smirnov (KS) test (http://www.physics.csbsju.edu/stats/KS-test.html). The KS test gives 95% confidence interval for the actual means. Based on the number of data points the KS statistic critical *D* value varies, which is the maximum difference between the cumulative distributions of two data sets. The critical values are $D_c = 0.168$ (for 63 events in cycle 23) and $D_c = 0.210$ (for 41 events in cycle 24). The KS statistical test results are given in Table 2. The resulting *D* value, 0.1178, is less than D_c indicating that the distributions are similar. The 95% confidence intervals of the means overlap (−73.33 and −66.87 nT for cycle 23 and −73.15 and −65.65 nT for cycle 24), again suggesting no significant difference between the distributions.

The solar source location of a CME plays a considerable role in deciding its geoeffectiveness. CMEs occurring near to the disk center are most likely to hit the Earth directly and cause storms [*Gopalswamy et al.*, 2007]. *Gopalswamy et al.* [2007] reported that the majority of 378 front side halo CMEs were geoeffective, and the geoeffectiveness decreased for CME source locations farther from the disk center. Figure 4 shows the CME source locations in heliospheric coordinates for the storms considered here. The moderate storms are differentiated using small (−50 to −75 nT) and large (−75 to −100 nT) circles. The two solar cycles are differentiated by the color of the circles. We determined the average *Dst* value for the disk CME (central meridian

Table 2. KS Test Result for Moderate Storm in SCs 23 and 24[a]

| Parameters | Solar Cycle 23 ($n = 63$) | | | Solar Cycle 24 ($n = 41$) | | | |
	Mean	Median	Confidence Intervals	Mean	Median	Confidence Intervals	D
Dst	−70.31	−68	−73.77 to −66.8	−70.32	−69	−73.15 to −65.6	0.1178
CME speed	716.3	562	602 to 830.4	668.8	561	538.1 to 799.5	0.11
B_z	−13.3	−12.52	−14.1 to −12.24	−12.44	−12.0	−13.6 to −11.6	0.288
VB_z	−5822	−5201	−6406 to −5238	−5490	−5180	−6001 to −4979	0.08

[a]Units of parameters: *Dst* and *Bz* in nT, CME speed in km/s, VB_z in km/s nT.
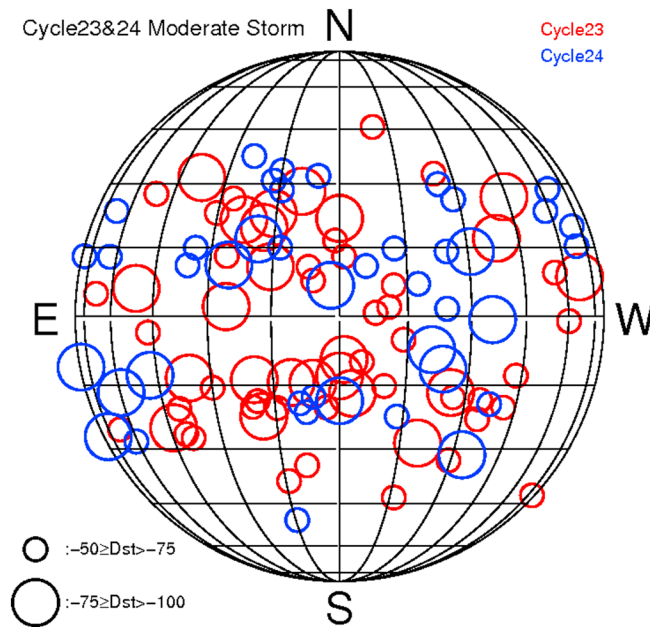
Figure 4. Solar source location of moderate storms occurred during SCs 23 and 24. The size difference in the circle indicates the strength of the *Dst* produced, and the range is mentioned in the figure. Red indicates the source location of SC 23, and blue denotes the cycle 24.

(CMD) within 30°) and nondisk CMEs (CMD > 30°). The averages are −72.4 nT for disk and −67.4 nT for nondisk CMEs in cycle 23; for cycle 24 they are −67.5 nT and −72.9 nT, respectively. These values do not show significant variation. Thus, moderate storms did not show any center-to-limb variation in the geoeffectiveness of CMEs. The average speed of limb CMEs is observed to be ~1100 km/s, whereas the nonlimb CMEs average speed is ~670 km/s in the sky plane. Although projection effects are expected, it appears that limb CMEs with higher CME speed are required to produce moderate storms.

3.2. CME Speed, Width, and Mass Distributions

Most of the geoeffective CMEs are halos; they mostly originate from close to the disk center. Out of the 63 storms in cycle 23, 32 (~50.7%) are due to halo CMEs, in solar cycle 24 is 20 out of 41 (or 48.7%) are due to halos. The fraction of halo CMEs in the two cycles are similar. The occurrence rate of all halo CMEs in cycles 23 and 24 is also similar [*Gopalswamy et al.*, 2014; *Gopalswamy et al.*, 2015a, 2015b]. The average CME speed for cycle 23 storms is ~716 km/s compared to ~ 671 km/s in cycle 24 (see Figure 5). Thus, there is only a 5% decrease in the average CME speeds; the difference is within the measurement errors. The CME speed distribution slightly broader in cycle 23: nearly 60% of the speeds are in the range of 300–900 km/s. The spread is narrower in cycle 24: ~75% of the CME speed values are in the range of 300–700 km/s. The maximum CME speed is ~2700 km/s (cycle 23) and ~ 2300 km/s (cycle 24), and both are halo CMEs. The 95% confidence intervals of the means obtained from the KS test overlapped (602 to 830 km/s in cycle 23 and 538 to 800 km/s in cycle 24), indicating no statistically insignificant differences in CME speeds between the two cycles. *Gopalswamy et al.* [2014] reported a decrease of 15% and 17% in MC and shock speeds, respectively, but the white light observations do not show any such change in average CME speeds for both the cycles.

We now consider the mass and width of CMEs, and the mass estimates are accurate to within a factor of 2. The disk center CME widths are likely to be affected by projection effects. Figure 6a shows the width distribution of CMEs associated with moderate storms in the two cycles. Halo CMEs represent the tallest bar in both the cycles. Excluding the halo CMEs, the average width is estimated to be 122° for solar cycle 23 and 141° for solar cycle (SC) 24. The nonhalo CME widths are consistent with the anomalous expansion of CME during cycle 24 when compared to the CME for cycle 23. But when the halo CMEs are included the average widths are similar (~245°). *Gopalswamy et al.* [2014, 2015a, 2015b] found an average width of 82.5° for cycle 23 compared to 98.1° for cycle 24 excluding halo CMEs and observed 93.4° for cycle 23 and 133.5° for solar cycle 24 when included. They reported an anomalous expansion of CME for cycle 24 when compared to solar cycle 23 for the same CME speed, but the criteria are different in their work, and only limb CMEs are considered along with that CMEs associated with solar flare c3 or larger. Limb CMEs are free from projection effect, but the moderate storms are mainly from the disk center and are subject to projection effects.

Figure 6b gives the distribution of CME masses for the two cycles. There are a few events in both the cycles for which the mass could not be measured using LASCO or STEREO and hence are excluded from the CME mass distribution. The average mass of CMEs associated with moderate storms in solar cycle 23 is 8.24×10^{15} g and 7.4×10^{15} g in cycle 24. Given the uncertainty in mass measurements, these values are not significantly
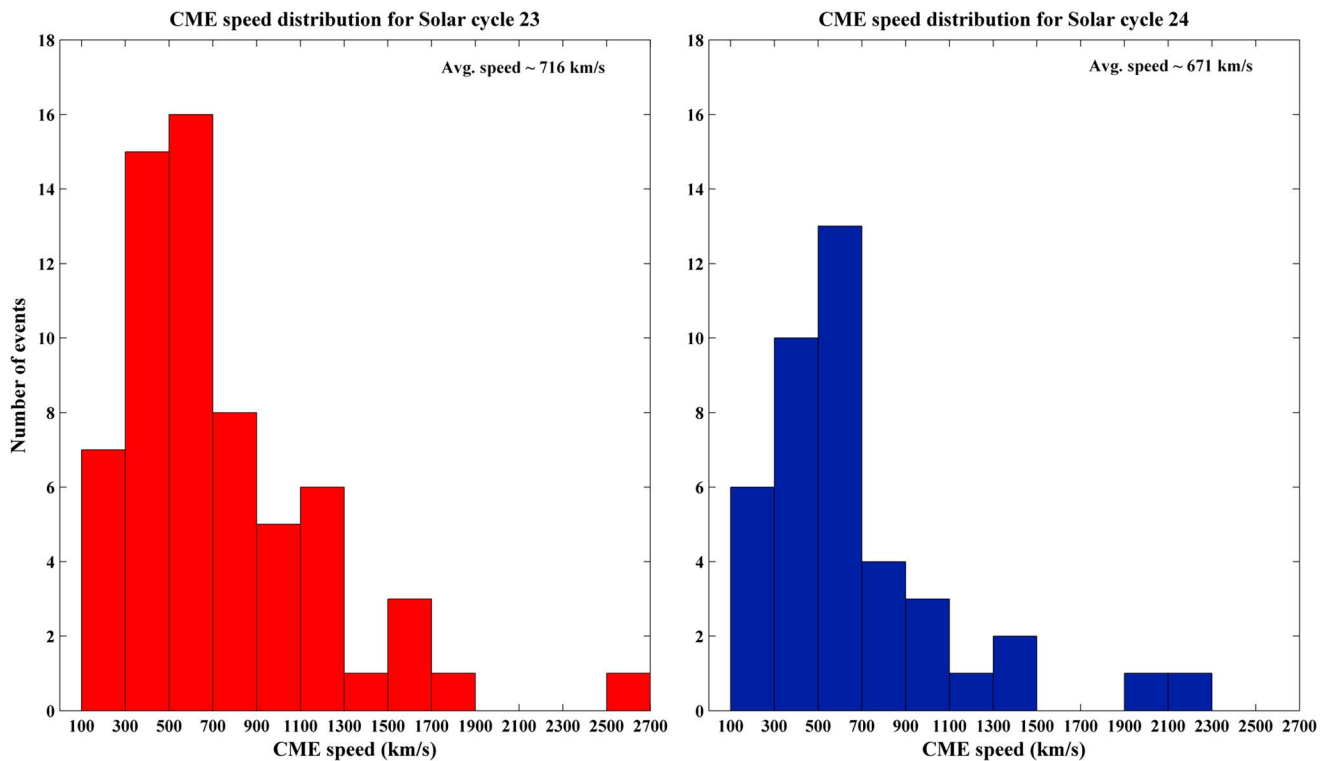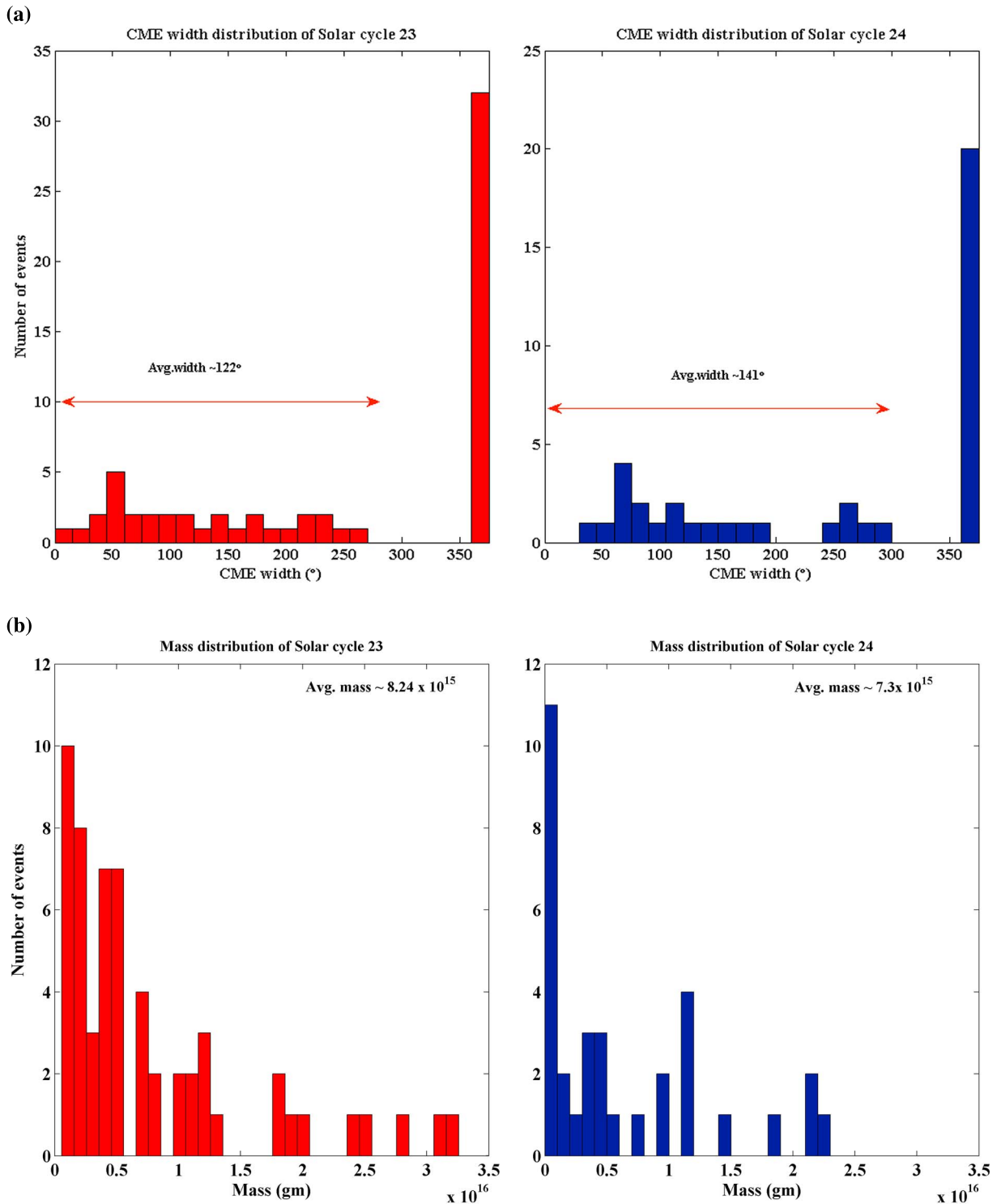
Figure 5. CME speed for moderate storm occurred during SCs 23 and 24.

different. The mass of limb CMEs during first 62 months of solar cycle 24 is decreased by a factor of 3 when compared to solar cycle 23 [*Gopalswamy et al.*, 2015b]. Also, the average CME mass during the whole of cycle 23 was found to be greater than that in cycle 24 [*Gopalswamy et al.*, 2010a; *Vourlidas et al.*, 2011]. But CMEs associated with moderate storms do not show much variation in mass.

3.3. Interplanetary and Magnetospheric Response

The main relation between CMEs and geomagnetic storms owes to the presence of negative B_z component of interplanetary magnetic field [*Gonzalez et al.*, 1994; *Zhang et al.*, 2007; *Gopalswamy*, 2008; *Echer et al.*, 2008a, 2008b, 2013; *Cid et al.*, 2012]. The negative B_z is not only found in CME flux ropes [*Wilson*, 1987] but also in the compressed sheath region between the flux rope and the shock [*Tsurutani et al.*, 1988; *Veenadhari et al.*, 2012]. The strength of a geomagnetic storm is proportional to the product VB_z, where V is the speed of the solar wind structure causing the storm. In addition to this, the ring current injection rate depends on VB_z along with the negative B_z duration and shock speed [*Balan et al.*, 2014; *Sandeep et al.*, 2015]. Since these two factors determine the geoeffectiveness, it is necessary to compare minimum B_z and VB_z between the cycles. At 1 AU, ICMEs can be differentiated as MC, nonmagnetic cloud or EJ and sheath based on the magnetic structure. In cycle 23, ~26.9% storms are caused by MC, ~49.2% by EJ, and 16% by sheath. Majority of the moderate storms are from nonmagnetic cloud in cycle 23. In cycle 24, the 41% of storms are caused by MCs, ~38% by EJs, and 21% by sheaths. The average Dst values for MC-associated moderate storms are ~73 nT in cycle 23 and ~65 nT for cycle 24. Although we restricted to a narrow range of Dst values, the results are in agreement with *Gopalswamy et al.* [2015b].

Figure 7 shows the distribution of minimum B_z and VB_z values for the storms in cycles 23 and 24. One moderate storm is not included in this statistics due to a OMNI data gap (10 November 2014). The B_z and VB_z values are taken from the region responsible for the Dst minimum, irrespective of MC, EJ, or sheath. The distribution of minimum B_z is longer in cycle 23 than that in cycle 24. The largest negative B_z observed is ~ −30 nT and ~ −20 nT for solar cycles 23 and 24, respectively. The smallest negative B_z is ~ −7 nT for both the cycles. The average B_z values are −13.2 nT in cycle 23 and −12.5 nT in cycle 24. A difference of 0.7 nT is

(a)

(b)

Figure 6. (a) Distribution of CME width of moderate storm occurred during SCs 23 and 24. (b) Distribution of CME mass of moderate storm occurred during SCs 23 and 24.

not significant. Figure 7 (right column) shows the distribution of computed VB_z for the storms. The largest negative value for cycle 23 is −14,082 km/s nT, and it is −9543 km/s nT for cycle 24. The average VB_z values in solar cycles 23 and 24 are −5822 km/s nT and −5890 km/s nT, respectively. These small variations are not significant. The KS test again shows overlap in the 95% confidence intervals for both B_z and VB_z.
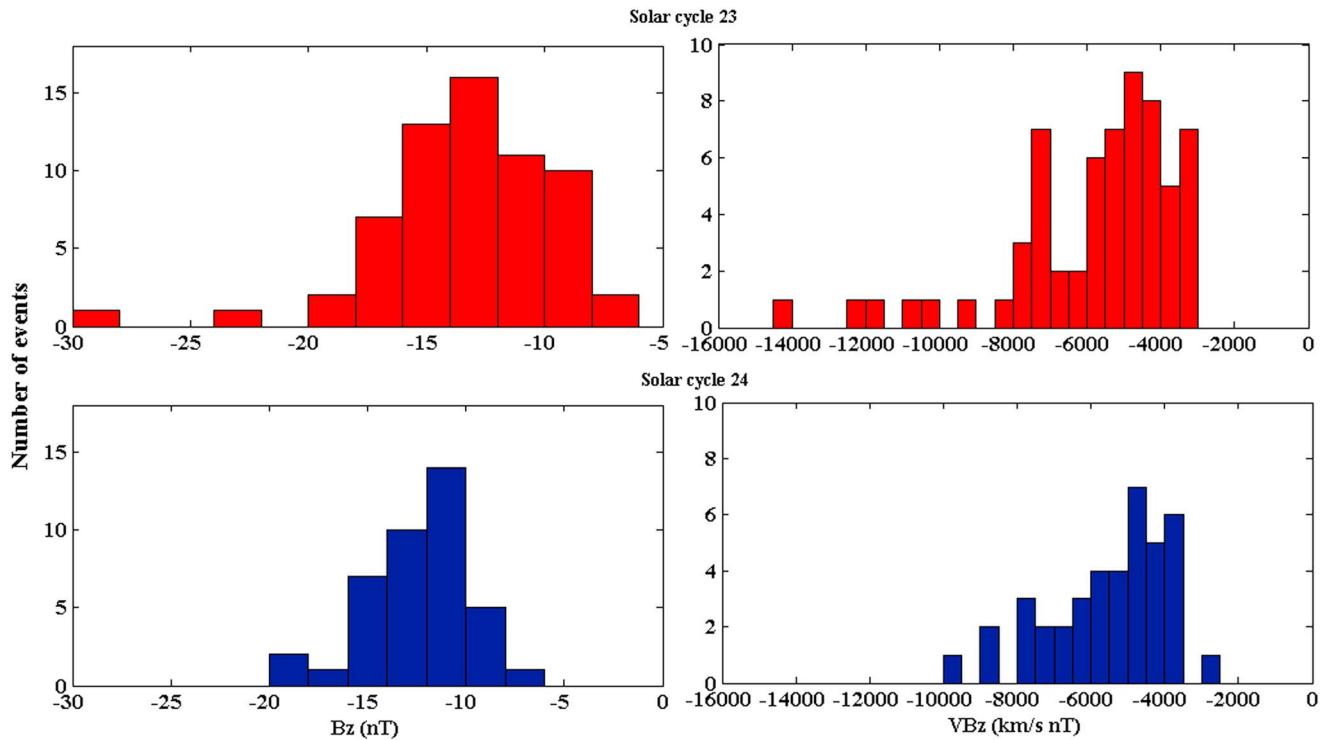
Figure 7. Distribution of B_z and VB_z for SCs (top row) 23 and (bottom row) 24 with respect to moderate storms.

Gopalswamy et al. [2015a] observed a declination of ~51% and ~40% in average VB_z with sheath and MC for solar cycle 24 when compared to 23, but in our work restriction of storm intensity (Dst) to a narrow range is expected to restrict the range of VB_z (and B_z) to similar values. *Gopalswamy et al.* [2014, 2015a] revealed the reduction in geoeffectiveness while considering total geoeffective CMEs. In the moderate storm case, the only indicator of reduced geoeffectiveness is the smaller number of moderate storms.

In order to see whether the Dst-VB_z relation holds for moderate storms, Dst is plotted against VB_z in Figure 8. The plot shows a linear variation with negative slopes for both the cycles. The correlation is found to be moderate with value of 0.68 for cycle 23 and 0.61 for cycle 24. Thus, the Dst-VB_z correlation did not change much. This means the storm process of converting solar wind energy to ring current energy did not change which is consistent with *Gopalswamy et al.* [2015a]. This correlation is statistically significant, and it is double the critical value of Pearson's correlation coefficient (for $P = 0.05$). The plot shows a few outliers in cycle 23 and a little more for cycle 24; this might be because the storm source is not differentiated among sheath, magnetic cloud, and nonmagnetic cloud that caused the Dst. In solar cycle 24 there was an extreme outlier due to the 29 June 2013 storm with a Dst of -98 nT with B_z -12.28 nT. In order to understand this discrepancy we examined the case separately. It was found that at 1 AU the CME was followed by an HSS with negative B_z, which made it last longer and resulted in a larger Dst magnitude.

In order to investigate the magnetospheric response during moderate storms, we performed a superposed epoch analysis of Dst and the associated interplanetary electric field (IEFy) for all the moderate storms that occurred during cycles 23 and 24. The results are shown in Figures 9a and 9b. The time 0 h (black line) in the figure indicates the main phase onset of all the moderate storms, and the dark blue line refers to the average Dst and IEFy. Figure 9c shows the average plot of Dst and IEFy obtained from the superposed epoch analysis. We see that the average minimum Dst stands out to be -58.7 nT for cycle 23 and -54.9 nT for cycle 24 with a difference of ~3.7 nT. The IEFy did not show much variation in their average values. The average time taken by the moderate storm to reach minimum Dst is less by 4 h for cycle 23 when compared to cycle 24. This delay suggests that although the average IEFy is similar, the response of the magnetosphere and the rate of ring current injection is rapid for cycle 23. This observation can be confirmed by evaluating the total energy
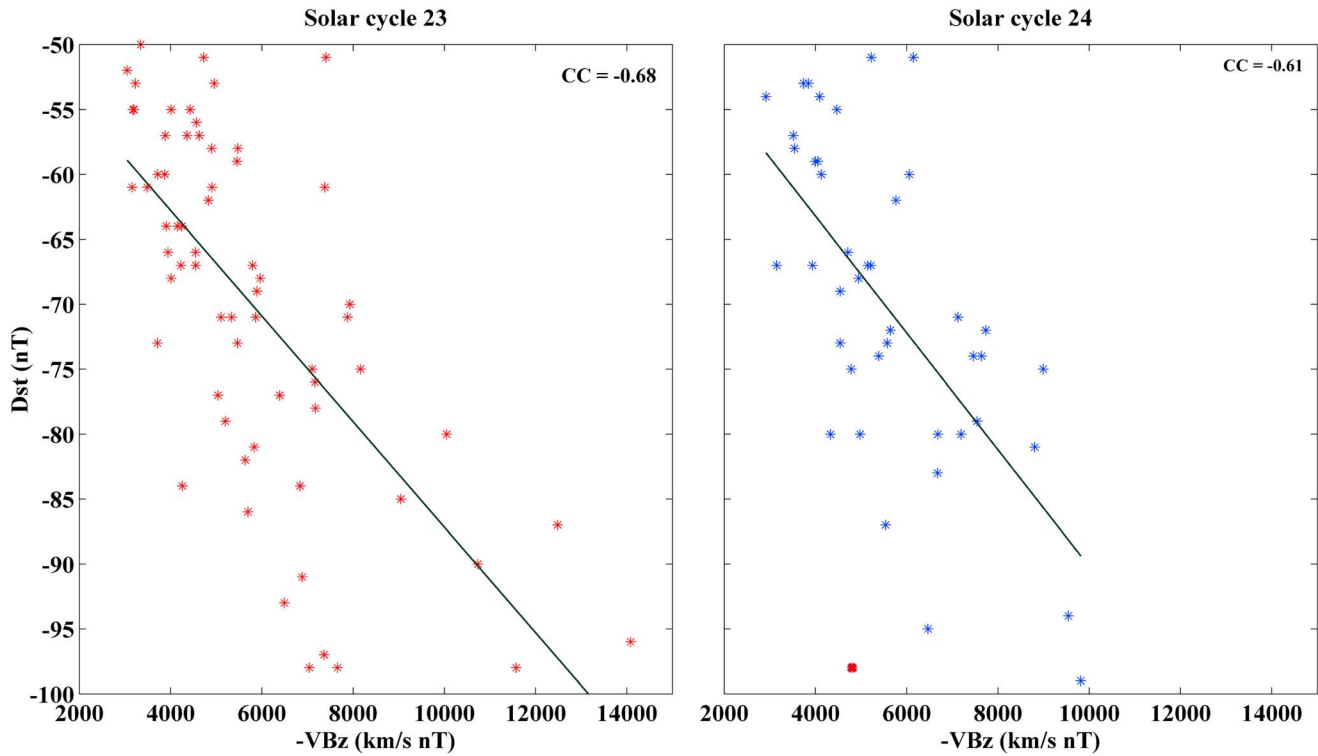
Figure 8. Correlation between *Dst* and *VB$_z$* for SCs 23 and 24.
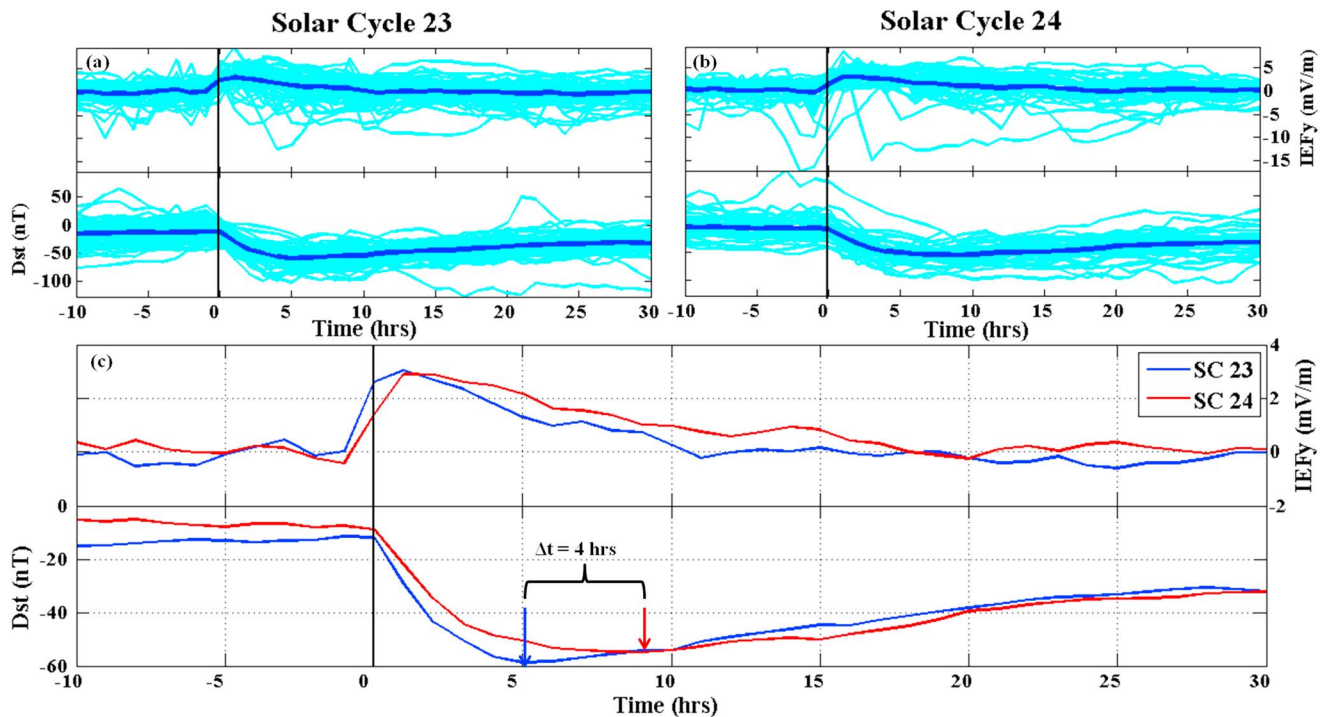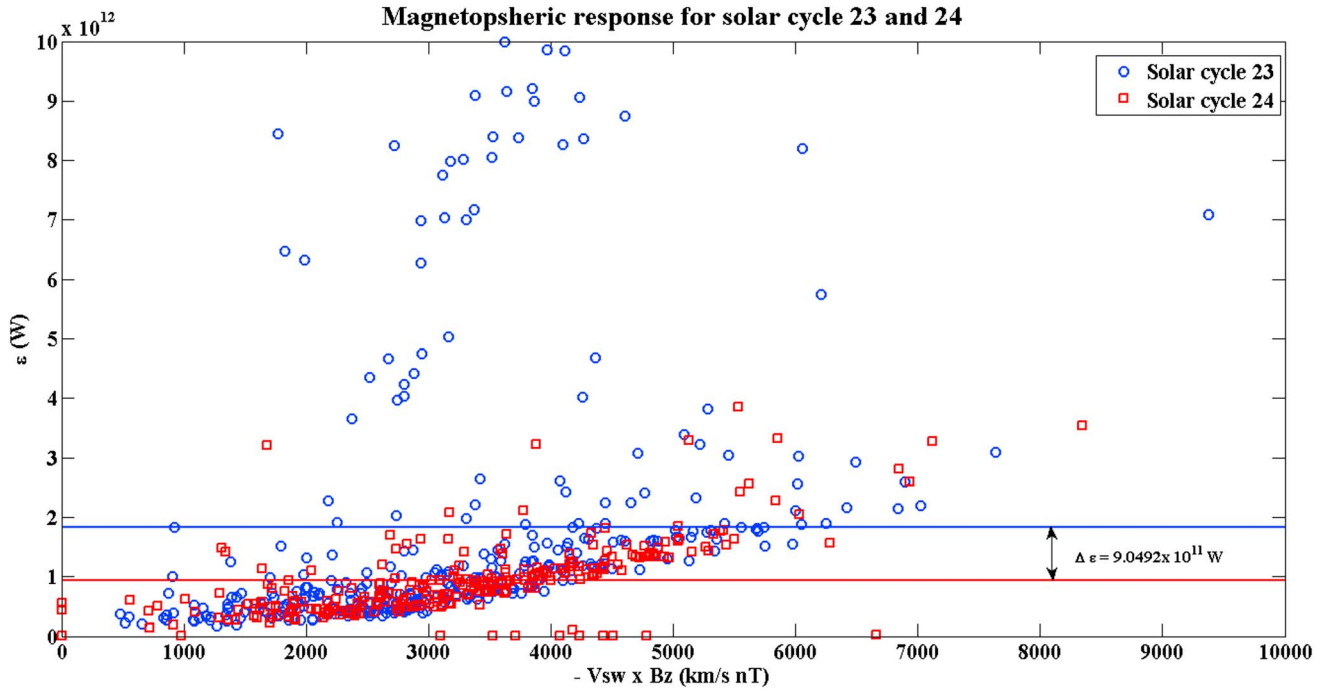

Figure 9. Superposed epoch plot of moderate storm *Dst* along with interplanetary electric field. (a) Solar cycle 23. (b) Solar cycle 24. (c) Average values of cycles 23 and 24.

Figure 10. The variation of ε with VB_z for solar cycles 23 and 24. Blue circle indicates cycle 23, and red square for cycle 24.

injected in to the magnetosphere for the two cycles. In order to check the response of magnetosphere, ε is estimated for the main phase of all moderate storms using the equation below.

$$\varepsilon = vB^2 \ \sin^4\left(\frac{\theta}{2}\right) R_{CF}^2 \tag{1}$$

where v is the upstream solar wind speed, B the magnitude of the IMF, and θ is the clock angle of IMF which is determined based on B_z values for $B_z < 0$

$$\theta = \ \tan^{-1}\left(\frac{|B_y|}{|B_z|}\right) \tag{2}$$

For $B_z > 0$

$$\theta = 180 - \tan^{-1}\left(\frac{|B_y|}{|B_z|}\right) \tag{3}$$

R_{CF} is determined by the below equation

$$R_{CF} = \left(\frac{B_0^2}{4\pi\rho v^2}\right)^{\frac{1}{6}} R_E \tag{4}$$

where B_0 is the magnetic field strength on the surface of the Earth equator.

ε gives the total energy transferred to the magnetosphere during the solar wind interaction [*Perrault and Akasofu*, 1978; *Nishida*, 1983]. R_{cf} is the distance at which the balance between solar wind kinetic plasma pressure and the magnetospheric magnetic pressure is obtained. We determined R_{cf} for all the moderate storms during the main phase and used it to estimate ε [*Holzer and Slavin*, 1979; *Sibeck et al.*, 1991]. Figure 10 shows the energy transfer during moderate storms as a function of VB_z for cycles 23 (blue) and 24 (red). Three events are excluded in solar cycle 23 due to unavailability of B_y required for calculating ε. The ε is estimated to be 1.83×10^{12} W for cycle 23 and 9.93×10^{11} W for cycle 24. So the average energy transfer is larger by 9.05×10^{11} W for cycle 23 than in cycle 24. Though VB_z is the same for the moderate storms the energy transfer is different. The difference in the energy transfer has led to main cause for delay in the minimum Dst during solar cycle 24, and a rapid main phase is observed in cycle 23.

4. Discussion

We compared the characteristics and sources of moderate storms between cycles 23 and 24. The first study about the interplanetary association of moderate storms is carried out by *Tsurutani and Gonzalez* [1997]. They studied the moderate storms occurred in solar maximum (1978–1979) of solar cycle 21 and reported that 40% of the storms were associated with ICME and remaining are due to HSS, CIR, and some phenomena related to Alfvenic fluctuations. Similarly, *Xu et al.* [2009] made a statistical study on the identification of interplanetary structure of moderate storms occurred during the period of 1998–2008 and found that nearly 51% of the moderate storms are due to ICMEs. This result is similar to our result that 68.2% of moderate storms are caused by ICMEs in cycle 23. The difference is clearly due to the consideration of different study periods, especially different phases of solar cycle.

Echer et al. [2013] found two peaks in the occurrence rate during the solar maximum and declining phases. Our results are consistent with this when the corresponding epochs are compared. They also reported that the CIR/HSS was the dominant source of moderate storms in the whole of cycle 23 which is opposite to our result. This discrepancy is attributed to the fact that *Echer et al.* [2013] included the declining phase of the solar cycle in which more CIR/HSS storms are known to occur. Our study does not include the declining phase. *Gopalswamy et al.* [2014] showed that the anomalous expansion diminished the magnetic content of CMEs in cycle 24, which in turn led to the reduction of large geomagnetic storms. Our result of ~75% reduction agrees well with this in case of intense storms, although the moderate storms are reduced only by 30%. Since CME width is proportional to the speed, CMEs producing major storms probably have a larger dilution of the CME magnetic content because they are faster. The number of halo CMEs among those causing moderate storms is similar in the cycle in agreement with *Gopalswamy et al.* [2015a].

Gopalswamy et al. [2015b] observed a cycle 23 to cycle 24 reduction of the *Dst* index associated to MCs: from −66 nT to −33 nT in the sheath portion and from −55 nT to −23 nT in the cloud portion. They estimated the reduction in geoeffectiveness by considering *Dst* values associated with the sheath and cloud portions. In our study we have considered MCs, non-MC, and their sheaths. Furthermore, we restricted the range of *Dst*, unlike *Gopalswamy et al.* [2015a]. These considerations reduced the difference between the two cycles. When MC-associated moderate storms are considered, there is a reduction in the average *Dst* values. The average mass of CMEs associated with moderate storms also did not show much variation between the two cycles. Whereas *Gopalswamy et al.* [2015a] found a reduction of CME mass by factor 3 in limb CMEs in solar cycle 24 when compared to cycle 23, it was not found in CMEs causing moderate storms. This is likely to be due to the fact that the CMEs associated with moderate storms are mostly disk events, for which the mass estimate is difficult. *Gopalswamy et al.* [2015b] also reported that CMEs had the same average speed in two cycles but not the width: a 33° increase in CME width was found for nonhalo limb CMEs in cycle 24. We found a change of 18°, but the average width did not show much change when halo CMEs are included. Again, the main difference is that our CMEs are subject to projection effects because they are mostly disk events, whereas *Gopalswamy et al.* [2015a] considered strictly limb events. We observed that limb CMEs with higher speeds are important to produce the moderate storms. But, as the limb CMEs have undergone anomalous expansion in cycle 24 (CMEs with flare C3 or greater) [*Gopalswamy et al.*, 2014], they could not produce moderate storms even with higher CME speeds.

The empirical relationship between *Dst* and VB_z for interplanetary magnetic structures cause storms [*Wu and Lepping*, 2002; *Gopalswamy et al.*, 2010a]. *Gopalswamy et al.* [2015a] obtained high correlation between *Dst* and VB_z for MCs in both cycles: correlation coefficients of 0.76 and 0.77 for the sheath and cloud portions in cycle 23 and 0.73 and 0.86 for cycle 24. We obtained moderate correlation between VB_z and *Dst* of 0.68 and 0.61 for solar cycles 23 and 24. The moderate correlation is due to the fact that we have included many storms driven by EJ and sheath portions of ICME. *Echer et al.* [2008a] have obtained the best correlation for solar cycle 23 intense storms: 0.80 for *Dst-Bs*, 0.84 for *Dst-Ey* (where *Ey* is electric field), and 0.55 for *Dst-V*$_{sw}$ (where V_{sw} is solar wind speed). For moderate storms, *Echer et al.* [2013] found a correlation coefficient of 0.55 between *Ey* and *Dst*, 0.48 between *Bs* and *Dst*, and negligible correlation between V_{sw} and *Dst*. We obtained a better correlation because of the fact that we have considered only CME-driven storms in which most of the cases have stable negative B_z and VB_z. The transfer of energy into the magnetosphere is less for cycle 23 than in cycle 24. As solar cycle 23 has undergone a long solar minimum, the background interplanetary condition in the cycle 24 has been low [*Kalegaev et al.*, 2014] similar to the weak heliospheric conditions.

As a result, the rate of magnetopsheric energy transfer and response of their current system is less for cycle 24 than the typical response in cycle 23 with the same interplanetary input. The CME with the optimum energy input which produced moderate storm in cycle 23 could not able to produce the same in cycle 24. So apart from the anomalous expansion of CMEs the energy distribution into the magnetosphere also played a major role in the reduction of moderate storms in solar cycle 24.

5. Conclusions

We investigated the solar source and the interplanetary characteristics of moderate geomagnetic storms that occurred during the first 77 months of solar cycles 23 and 24. We find that the distribution of CME speed and average mass is almost the same in both the cycles, whereas slight variation was observed in average width of nonhalo CMEs. The Dst values of moderate storms did not show considerable change with the source location of the CMEs in the two cycles. The minimum B_z values showed a wider distribution in cycle 23 when compared to cycle 24. The highest correlation is obtained between VB_z and Dst for both the cycles, a property universal to storms of all strength. From the statistical analysis, we find that moderate storms did not show much change when compared to cycle 23. This is because the restricted Dst range restricts the range of VB_z. The reduced geoeffectiveness in cycle 24 is mainly due to the decrease in the intense storms and to a smaller extent in the number of moderate storms, which is the resultant of anomalous CME expansion and less magnetopsheric energy transfer in cycle 24.

The main conclusions are as follows.

1. A total of 166 geomagnetic storms (intense + moderate) are identified during the first 77 months of solar cycle 23 and 67 in cycle 24 over the same epoch. The number of moderate storms is 111 and 55 in cycles 23 and 24, respectively. Solar cycle 24 has shown nearly 80% reduction in the occurrence of intense storms, whereas it is only 40% in the case of moderate storms (from Figure 1 and Table 1).
2. The occurrence of moderate storms approximately follows the SSN and peaks around the solar maximum for both the cycles (from Figure 2).
3. Average CME speed and Dst values do not show much variation in the two cycles (from Figures 3 and 5). Similarly, average CME mass did not show much variation, whereas the CME width has shown a slight variation for nonhalo CMEs when compared to cycle 23 (From Figures 6a and 6b).
4. The correlation between VB_z and Dst is found to be the highest with values of 0.68 for cycle 23 and 0.61 for cycle 24 (from Figure 8).
5. The magnetospheric energy transfer decreased in solar cycle 24 with respect to that in cycle 23 (from Figure 10).

References

Alex, S., S. Mukherjeea, and G. S. Lakhina (2006), Geomagnetic signatures during the intense geomagnetic storms of 29 October and 20 November 2003, *J. Atmos. Sol. Terr. Phys.*, 68, 769–780, doi:10.1016/j.jastp.2006.01.003.

Alexeev, I. I., E. S. Belenkaya, V. V. Kalegaev, Y. I. Feldstein, and A. Grafe (1996), Magnetic storms and magnetotail currents, *J. Geophys. Res.*, 101, 7737–7747, doi:10.1029/95JA03509.

Balan, N., R. Skoug, S. Tulasi Ram, P. K. Rajesh, K. Shiokawa, Y. Otsuka, I. S. Batista, and T. Nakamura (2014), CME front and severe space weather, *J. Geophys. Res. Space Physics*, 119, 10,041–10,058, doi:10.1002/2014JA020151.

Berdichevsky, D. B., C. J. Farrugia, B. J. Thompson, R. P. Lepping, D. V. Reames, M. L. Kaiser, J. T. Steinberg, S. P. Plunkett, and D. J. Michels (2002), Halo-coronal mass ejections near the 23rd solar minimum: Liftoff, inner heliosphere, and in situ (1 AU) signatures, *Ann. Geophys.*, 20, 891–916, doi:10.5194/angeo-20-891-2002.

Brueckner, G. E., J.-P. Delaboudiniere, R. A. Howard, S. E. Paswaters, O. C. S. Cyr, R. Schwenn, P. Lamy, G. M. Simnett, B. Thompson, and D. Wang (1998), Geomagnetic storms caused by coronal mass ejections (CMEs): March 1996 through June 1997, *Geophys. Res. Lett.*, 25, 3019–3022, doi:10.1029/98GL00704.

Chapman, S., and J. Bartels (1940), *Geomagnetism*, vol. I, chap. IX, Clarendon, Oxford.

Cid, C., et al. (2012), Can a halo CME from the limb be geoeffective?, *J. Geophys. Res.*, 117, A11102, doi:10.1029/2012JA017536.

Daglis, I. A., and R. M. Thorne (1999), The terrestrial ring current: Origin, formation, and decay, *Rev. Geophys.*, 37, 407–438, doi:10.1029/1999RG900009.

Dal Lago, A., et al. (2004), Great geomagnetic storms in the rise and maximum of solar cycle 23, *Braz. J. Phys.*, 34, 1542–1546, doi:10.1590/S0103-97332004000800008.

Dungey, J. W. (1961), Interplanetary magnetic field and the auroral zones, *Phys. Rev. Lett.*, 6, 47–48, doi:10.1103/PhysRevLett.6.47.

Echer, E., W. D. Gonzalez, F. L. Guarnieri, A. Dal Lago, and L. E. A. Vieira (2005), Introduction to space weather, *Adv. Space Res.*, 35, 855–865, doi:10.1016/j.asr.2005.02.098.

Echer, E., W. D. Gonzalez, and B. T. Tsurutani (2008a), Interplanetary conditions leading to superintense geomagnetic storms ($Dst < -250$) during solar cycle 23, *Geophys. Res. Lett.*, 35, L06S03, doi:10.1029/2007GL031755.

Echer, E., W. D. Gonzalez, B. T. Tsurutani, and A. L. C. Gonzalez (2008b), Interplanetary conditions causing intense geomagnetic storms ($Dst \leq -100$ nT) during solar cycle 23 (1996–2006), *J. Geophys. Res.*, *113*, A05221, doi:10.1029/2007JA012744.

Echer, E., W. D. Gonzalez, and B. T. Tsurutani (2011), Statistical studies of geomagnetic storms with peak $Dst \leq \_50$ nT from 1957 to 2008, *J. Atmos. Sol. Terr. Phys.*, *73*, 1454–1459, doi:10.1016/j.jastp.2011.04.021.

Echer, E., B. T. Tsurutani, and W. D. Gonzalez (2013), Interplanetary origins of moderate (-100 nT $< Dst \leq -50$ nT) geomagnetic storms during solar cycle 23 (1996–2008), *J. Geophys. Res. Space Physics*, *118*, 385–392, doi:10.1029/2012JA018086.

Gonzalez, W. D., and B. T. Tsurutani (1987), Criteria of interplanetary parameters causing intense magnetic storms ($Dst < \_100$ nT), *Planet. Space Sci.*, *35*, 1101, doi:10.1016/0032-0633(87)90015-8.

Gonzalez, W. D., and E. Echer (2005), A study on the peak Dst and peak negative B_z relationship during intense geomagnetic storms, *Geophys. Res. Lett.*, *32*, L18103, doi:10.1029/2005GL023486.

Gonzalez, W. D., J. A. Joselyn, Y. Kamide, H. W. Kroehl, G. Rostoker, B. T. Tsurutani, and V. Vasyliunas (1994), What is a geomagnetic storm, *J. Geophys. Res.*, *99*, 5771–5792, doi:10.1029/93JA02867.

Gonzalez, W. D., B. T. Tsurutani, and A. L. Clua de Gonzalez (1999), Interplanetary origin of geomagnetic storms, *Space Sci. Rev.*, *88*, 529–562, doi:10.1023/A:1005160129098.

Gonzalez, W. D., E. Echer, A. L. Clua-Gonzalez, and B. T. Tsurutani (2007), Interplanetary origin of intense geomagnetic storms ($Dst < -100$ nT) during solar cycle 23, *Geophys. Res. Lett.*, *34*, L06101, doi:10.1029/2006GL028879.

Gonzalez, W. D., E. Echer, B. T. Tsurutani, A. L. Clua de Gonzalez, and A. Dal Lago (2011), Interplanetary origin of intense, superintense and extreme geomagnetic storms, *Space Sci. Rev.*, *158*, 69–89.

Gopalswamy, N. (2008), Solar connections of geoeffective magnetic structures, *J. Atmos. Sol. Terr. Phys.*, *70*, 7028.

Gopalswamy, N. (2010), The CME link to geomagnetic storms, in *Proceedings of the IAU Symposium*, vol. 264, edited by A. G. Kosovichev, A. H. Andrei, and J.-P. Rozelot, pp. 326–335, Cambridge Univ. Press, Cambridge, U. K.

Gopalswamy, N., S. Yashiro, and S. Akiyama (2007), Geoeffectiveness of halo coronal mass ejections, *J. Geophys. Res.*, *112*, A06112, doi:10.1029/2006JA012149.

Gopalswamy, N., S. Yashiro, G. Michalek, G. Stenborg, A. Vourlidas, S. Freeland, and R. A. Howard (2009), The SOHO/LASCO CME catalog, *Earth Moon Planets*, *104*, 295–313.

Gopalswamy, N., H. Xie, P. Mäkelä, S. Akiyama, S. Yashiro, M. L. Kaiser, R. A. Howard, and J. L. Bougeret (2010a), Interplanetary shocks lacking type II radio bursts, *Astrophys. J.*, *710*, 1111, doi:10.1088/0004-637X/710/2/1111.

Gopalswamy, N., S. Yashiro, G. Michalek, H. Xie, P. Mäkelä, A. Vourlidas, and R. A. Howard (2010b), A catalog of halo coronal mass ejections from SOHO, *Sun Geosphere*, *5*(1), 7–16.

Gopalswamy, N., S. Yashiro, P. Mäkelä, G. Michalek, K. Shibasaki, and D. H. Hathaway (2012), Behavior of solar cycles 23 and 24 revealed by microwave observations, *Astrophys. J.*, *750*, LL42, doi:10.1088/2041-8205/750/2/L42.

Gopalswamy, N., S. Akiyama, S. Yashiro, H. Xie, P. Mäkelä, and G. Michalek (2014), Anomalous expansion of coronal mass ejections during solar cycle 24 and its space weather implications, *Geophys. Res. Lett.*, *41*, 2673–2680, doi:10.1002/2014GL059858.

Gopalswamy, N., B. Tsurutani, and Y. Yan (2015a), Short-term variability of the Sun-Earth system: An overview of progress made during the CAWSES II period, *Prog. Earth Planet. Sci.*, *2*, 13, doi:10.1186/s40645-015-0043-8.

Gopalswamy, N., S. Yashiro, H. Xie, S. Akiyama, and P. Mäkelä (2015b), Properties and geoeffectiveness of magnetic clouds during solar cycles 23 and 24, *J. Geophys. Res. Space Physics*, *120*, 9221–9245, doi:10.1002/2015JA021446.

Gosling, J. T. (1996), Corotating and transient solar wind flows in three dimensions, *Annu. Rev. Astron. Astrophys.*, *34*, 35–73, doi:10.1146/annurev.astro.34.1.35.

Gosling, J. T., and V. J. Pizzo (1999), Formation and evolution of corotating interaction regions and their three dimensional structure, *Space Sci. Rev.*, *89*, 21–52, doi:10.1023/A:1005291711900.

Gosling, J. T., D. J. McComas, J. L. Phillips, and S. J. Bame (1991), Geomagnetic activity associated with Earth passage of interplanetary shock disturbances and coronal mass ejections, *J. Geophys. Res.*, *96*, 7831–7839, doi:10.1029/91JA00316.

Holzer, R. E., and J. A. Slavin (1979), Magnetic flux transfer associated with expansions and contractions of the dayside magnetosphere, *J. Geophys. Res.*, *83*, 3831–3839, doi:10.1029/JA083iA08p03831.

Hutchinson, J. A., D. M. Wright, and S. E. Milan (2011), Geomagnetic storms over the last solar cycle: A superposed epoch analysis, *J. Geophys. Res.*, *116*, A09211, doi:10.1029/2011JA016463.

Kalegaev, V. V., I. I. Alexeev, I. S. Nazarkov, V. Angelopoulos, and A. Runov (2014), On the large-scale structure of the tail current as measured by THEMIS, *Adv. Space Res.*, *54*, 1773–1785, doi:10.1016/j.asr.2014.07.019.

Kilpua, E. K. J., J. G. Luhmann, L. K. Jian, C. T. Russell, and Y. Li (2014), Why have geomagnetic storms been so weak during the recent solar minimum and the rising phase of cycle 24?, *J. Atmos. Sol. Terr. Phys.*, *107*(2014), 12–19, doi:10.1016/j.jastp.2013.11.001.

Klein, L. W., and L. F. Burlaga (1982), Interplanetary magnetic clouds at 1 AU, *J. Geophys. Res.*, *87*, 613–624, doi:10.1029/JA087iA02p00613.

Lean, J. L., S. E. McDonald, J. D. Huba, J. T. Emmert, D. P. Drob, and C. L. Siefring (2014), Geospace variability during the 2008–2009 whole heliosphere intervals, *J. Geophys. Res. Space Physics*, *119*, 3755–3776, doi:10.1002/2013JA019485.

Liemohn, M. W., J. U. Kozyra, M. F. Thomsen, J. L. Roeder, G. Lu, J. E. Borovsky, and T. E. Cayton (2001), Dominant role of the asymmetric ring current in producing the stormtime Dst^*, *J. Geophys. Res.*, *106*, 10,883–10,904, doi:10.1029/2000JA000326.

Lopez, R. E., W. D. Gonzalez, V. Vasyliūnas, I. G. Richardson, C. Cid, E. Echer, G. D. Reeves, and P. C. Brandt (2015), Decrease in SYM-H during a storm main phase without evidence of a ring current injection, *J. Atmos. Sol. Terr. Phys.*, *134*, 118–129, doi:10.1016/j.jastp.2015.09.016.

Mac-Mahon, R. M., and W. D. Gonzalez (1997), Energetics during the main phase of geomagnetic superstorms, *J. Geophys. Res.*, *102*, 14,199–14,207, doi:10.1029/97JA01151.

Mursula, K., and B. Zieger (1996), The 13.5-day periodicity in the Sun, solar wind, and geomagnetic activity: The last three solar cycles, *J. Geophys. Res.*, *101*, 27,077–27,090, doi:10.1029/96JA02470.

Nishida, A. (1983), IMF control of the Earth's magnetosphere, *Space Sci. Rev.*, *34*, 185–200, doi:10.1007/BF00194626.

Perrault, P., and S. I. Akasofu (1978), A study of magnetic storms, *Geophys. J. R. Astron. Soc.*, *54*, 547–573, doi:10.1111/j.1365-246X.1978.tb05494.x.

Potgieter, M. S., E. E. Vos, M. Boezio, N. De Simone, V. Di Felice, and V. Formato (2014), Modulation of galactic protons in the heliosphere during the unusual solar minimum of 2006 to 2009, *Sol. Phys.*, *289*, 391–406.

Richardson, I. G., H. V. Cane, and E. W. Cliver (2002), Sources of geomagnetic activity during nearly three solar cycles (1972–2000), *J. Geophys. Res.*, *107*(A8), 1187, doi:10.1029/2001JA000504.

Richardson, I., and H. V. Cane (2010), Near-Earth interplanetary coronal mass ejections during solar cycle 23 (1996–2009): Catalog and summary of properties, *Sol. Phys.*, *264*(1), 189–237, doi:10.1007/s11207-010-9568-6.

Riley, P., and I. G. Richardson (2012), Using statistical multivariable models to understand the relationship between interplanetary coronal mass ejecta and magnetic flux ropes, *Sol. Phys.*, *012*, 6–9.

Sandeep, K., B. Veenadhari, S. Tulasi Ram, R. Selvakumaran, S. Mukherjee, S. Rajesh, and B. D. Kadam (2015), Estimation of interplanetary electric field conditions for historical geomagnetic storms, *J. Geophys. Res. Space Physics*, *120*, 7307–7317, doi:10.1002/2015JA021661.

Sibeck, D. G., R. E. Lopez, and E. C. Roelof (1991), Solar wind control of the magnetopause shape, location and motion, *J. Geophys. Res.*, *96*, 5489–5495, doi:10.1029/90JA02464.

Smith, E. J., and J. H. Wolf (1976), Observations of interaction regions and corotating shocks between one and five AU: Pioneers 10 and 11, *Geophys. Res. Lett.*, *3*, 137–140, doi:10.1029/GL003i003p00137.

Solomon, S. C., L. Qian, and A. G. Burns (2013), The anomalous ionosphere between solar cycles 23 and 24, *J. Geophys. Res. Space Physics*, *118*, 6524–6535, doi:10.1002/jgra.50561.

Sugiura, M. (1964), Hourly values of equatorial *Dst* for the IGY, *Ann. Int. Geophys. Year*, *35*, 9–45.

Sugiura, M., and S. Chapman (1960), The average morphology of geomagnetic storms with sudden commencement, A bandl. Akad. Wiss., Gottingen Math. Phys. K1 (4), 1960.

Tsurutani, B. T., and W. D. Gonzalez (1997), The interplanetary causes of magnetic storms: A review, in *Magnetic Storms*, *Geophys. Monogr. Ser.*, vol. 98, edited by B. T. Tsurutani et al., pp. 77–89, AGU, Washington, D. C.

Tsurutani, B. T., W. D. Gonzalez, F. Tang, S. I. Akasofu, and E. J. Smith (1988), Origin of interplanetary southward magnetic fields responsible for major magnetic storms near solar maximum (1978–1979), *J. Geophys. Res.*, *93*, 8519–8531, doi:10.1029/JA093iA08p08519.

Tsurutani, B. T., W. D. Gonzalez, F. Tang, and Y. T. Lee (1992), Great magnetic storms, *Geophys. Res. Lett.*, *19*, 73–76, doi:10.1029/91GL02783.

Tsurutani, B. T., W. D. Gonzalez, A. L. C. Gonzalez, F. Tang, J. Arballo, and M. Okada (1995), Interplanetary origin of geomagnetic activity in the declining phase of the solar cycle, *J. Geophys. Res.*, *100*(A11), 21,717–21,733, doi:10.1029/95JA01476.

Tsurutani, B. T., R. L. McPherron, W. D. Gonzalez, G. Lu, N. Gopalswamy, and F. L. Guarnieri (2006), Magnetic storms caused by corotating solar wind streams, AGU Monograph 167, Recurrent magnetic storms, corotating solar wind streams.

Tsurutani, B. T., E. Echer, F. L. Guarnieri, and W. D. Gonzalez (2011), The properties of two solar wind high speed streams and related geomagnetic activity during the declining phase of solar cycle 23, *J. Atmos. Sol. Terr. Phys.*, *73*, 164–177, doi:10.1016/j.jastp.2010.04.003.

Turner, N. E., D. N. Baker, T. I. Pulkkinen, and R. L. McPherron (2000), Evaluation of the tail current contribution to *Dst*, *J. Geophys. Res.*, *105*, 5431–5439, doi:10.1029/1999JA000248.

Veenadhari, B., R. Selvakumaran, R. Singh, A. K. Maurya, N. Gopalswamy, S. Kumar, and T. Kikuchi (2012), Coronal mass ejection-driven shocks and the associated sudden commencements/sudden impulses, *J. Geophys. Res.*, *117*, A04210, doi:10.1029/2011JA017216.

Vourlidas, C. A., R. A. Howard, E. Esfandiari, S. Patsourakos, S. Yashiro, and G. Michalek (2011), Erratum: "Comprehensive analysis of coronal mass ejection mass and energy properties over a full solar cycle" (2010, Astrophys J 722, 1522), *Astrophys. J.*, *730*, 59, doi:10.1088/0004-637X/730/1/59.

Wang, C. B., J. K. Chao, C.-H. Lin (2003), Influence of the solar wind dynamic pressure on the decay and injection of the ring current. *J. Geophys. Res.*, *108*(A9), 1341, doi:10.1029/2003JA009851.

Webb, D. F. (1991), The solar cycle variation of the rates of CMEs and related activity, *Adv. Space Res.*, *11*, 37–40, doi:10.1016/0273-1177(91)90086-Y.

Webb, D. F., N. U. Crooker, S. P. Plunkett, and O. C. S. Cyr (2001), The solar sources of geoeffective structures, in *Space Weather*, *Geophys. Monogr. Ser.*, vol. 125, edited by S. Paul, J. S. Howard, and L. S. George, pp. 123–142, AGU, Washington, D. C.

Weiss, L. A., P. H. Reif, J. J. Moses, B. D. Moore, and R. A. Heelis (1992), Energy dissipations in substorms, Eur. Space Agency Spec. Pub., ESA-SP-335,309-319.

Wilson, R. M. (1987), Geomagnetic response to magnetic clouds, *Planet. Space Sci.*, *33*, 329, doi:10.1016/0032-0633(87)90159-0.

Wu, C., and R. P. Lepping (2002), Effects of magnetic clouds on the occurrence of geomagnetic storms: The first 4 years of Wind, *J. Geophys. Res.*, *107*(A10), 1314, doi:10.1029/2001JA000161.

Xu, D., T. Chen, X. X. Zhang, and Z. Liu (2009), Statistical relationship between solar wind conditions and geomagnetic storms in 1998–2008, *Planet. Space Sci.*, *57*, 1500–1513, doi:10.1016/j.pss.2009.07.015.

Yashiro, S., N. Gopalswamy, G. Michalek, O. C. S. Cyr, S. P. Plunkett, N. B. Rich, and R. A. Howard (2004), A catalog of white light coronal mass ejections observed by the SOHO spacecraft, *J. Geophys. Res.*, *109*, A07105, doi:10.1029/2003JA010282.

Zhang, J., K. P. Dere, R. A. Howard, and V. Bothmer (2003), Identification of solar sources of major geomagnetic storms between 1996 and 2000, *Astrophys. J.*, *582*, 520–533, doi:10.1086/344611.

Zhang, J., M. W. Liemonh, J. U. Kozyra, M. F. Thomsen, H. A. Elliott, and J. M. Weygand (2006), A statistical comparison of solar wind sources of moderate and intense geomagnetic storms at solar minimum and maximum, *J. Geophys. Res.*, *111*, A01104, doi:10.1029/2005JA011065.

Zhang, J., et al. (2007), Solar and interplanetary sources of major geomagnetic storms (*Dst* < 100 nT) during 1996–2005, *J. Geophys. Res.*, *112*, A10102, doi:10.1029/2007JA012321.